Qualitative and numerical analysis of the Rössler model: Bifurcations of equilibria

R. Barrio [a,*], F. Blesa [b], A. Dena [c], S. Serrano [a]

[a] Depto. Matemática Aplicada, GME and IUMA, Universidad de Zaragoza, E-50009 Zaragoza, Spain
[b] Depto. Física Aplicada and GME, Universidad de Zaragoza, E-50009 Zaragoza, Spain
[c] Centro Universitario de la Defensa, Academia General Militar, E-50090 Zaragoza, Spain

A B S T R A C T

In this paper, we show the combined use of analytical and numerical techniques in the study of bifurcations of equilibria of low-dimensional chaotic problems. We study in detail different aspects of the paradigmatic Rössler model. We provide analytical formulas for the stability of the equilibria as well as some of their codimension one, two, and three bifurcations. In particular, we carry out a complete study of the Andronov–Hopf bifurcation, establishing explicit formulas for its location and studying its character numerically, determining a curve of generalized-Hopf bifurcation, where the Hopf bifurcation changes from subcritical to supercritical. We also briefly study some routes among the different Andronov–Hopf bifurcation curves and how these routes are influenced by the local and global bifurcations of limit cycles. Finally, we show the U-shape of the homoclinic bifurcation curve at the studied parameter values.

Keywords:
Rössler equations, Bifurcations of equilibria, Hopf bifurcation.

1. Introduction

The Rössler model [1] is a paradigmatic problem among low-dimensional dynamical systems with chaotic behavior. So, a large number of articles [2–11] are still being published giving new partial results. However, this problem is not yet fully understood. The importance of this system, together with the Lorenz model, is that, being paradigmatic problems, they have become test problems for almost all new analytical and numerical techniques in computational dynamics.

The Rössler equations [1] are given by

$$\begin{aligned} \dot{x} &= -(y+z), \\ \dot{y} &= x + ay, \\ \dot{z} &= b + z(x-c), \end{aligned} \tag{1}$$

with $a, b, c \in \mathbb{R}$, and they are assumed to be positive and dimensionless.

The main goal of the present paper is to show how the use of numerical and analytical techniques can provide complete qualitative studies for low-dimensional chaotic problems, in particular in the study of bifurcations of equilibria. We focus our attention on the Rössler system in order to provide complete explicit expressions for the location and stability of the different equilibria, as well as for the Andronov–Hopf bifurcations. For the complete study of this bifurcation we need some numerical explorations due to the high complexity in the analysis of the codimension two bifurcations when the

* Corresponding author.
E-mail addresses: rbarrio@unizar.es (R. Barrio), fblesa@unizar.es (F. Blesa), adena@unizar.es (A. Dena), sserrano@unizar.es (S. Serrano).

first Lyapunov coefficient vanishes. Also, we show how the global homoclinic bifurcations give rise to different routes in the connection via limit cycles between the different bifurcation curves in the space of parameters.

The paper is organized as follows. In Section 2, we provide analytical formulas for the stability of the equilibria. In Section 3, we present some codimension one, two, and three bifurcations of equilibria [12], in particular, a complete study of the Andronov–Hopf bifurcation is performed. In Section 4, we study different routes among the Hopf bifurcation curves and we show the connection among the bifurcation curves of equilibria, limit cycles, and the chaotic and regular regions, and we show the U-shape of the homoclinic bifurcation curve. Finally, in Section 5, we present some conclusions.

2. Equilibria: location and stability

Some of the first data to obtain in the analysis of a dynamical system are the equilibrium points and their bifurcations. The Rössler equations have two equilibrium points [7] for $c^2 > 4ab$, given by $P_1 = (-ap_1, p_1, -p_1)$ and $P_2 = (-ap_2, p_2, -p_2)$, with

$$p_1 := \frac{1}{2}\left(-\frac{c}{a} - \frac{\sqrt{c^2-4ab}}{a}\right), \qquad p_2 := \frac{1}{2}\left(-\frac{c}{a} + \frac{\sqrt{c^2-4ab}}{a}\right).$$

If $c^2 = 4ab$, then $P_1 = P_2$.

The stability of the equilibrium points can be studied analytically by means of the classical Routh–Hurwitz criterion, but in the literature there are only partial answers without explicit equations for the stable regions.

Proposition 1. *The equilibrium point P_1 in the Rössler system is always unstable and P_2 is linearly stable iff the parameters a, c belong to $S_1 = \{(a,c)|a \le 1 \text{ and } c > 2a\}$ or to $S_2 = \{(a,c)|a \in (1,\sqrt{2}) \text{ and } c \in (2a, 2a/(a^2-1))\}$, and the parameter b satisfies*

$$b_H(a,c) \le b < b_E(a,c), \tag{2}$$

with

$$\begin{aligned} b_E(a,c) &:= \frac{c^2}{4a}, \\ b_H(a,c) &:= \frac{a\left(2 - a^4 + ca^3 + 2a^2 - ca + c^2 + (c-a)\sqrt{a^6 - 4a^4 + 2ca^3 - 4a^2 + c^2}\right)}{2\left(a^2+1\right)^2}. \end{aligned} \tag{3}$$

Proof. The proof is obtained by using the Routh–Hurwitz criterion (RHC). The RHC applied to a polynomial of degree 3, $x^3 + Ax^2 + Bx + C$, requires that $C > 0, A > 0$, and $AB > C$. Taking the linearized equations around both equilibrium points permits us to obtain their characteristic polynomials. For P_1 and P_2, respectively,

$$\begin{aligned} q_1(x) &= x^3 + \frac{c - 2a - K}{2}x^2 + \frac{2a + c - a^2c + (1+a^2)K}{2a}x - K, \\ q_2(x) &= x^3 + \frac{c - 2a + K}{2}x^2 + \frac{2a + c - a^2c - (1+a^2)K}{2a}x + K, \end{aligned}$$

with $K = \sqrt{c^2 - 4ab}$. The point P_1 already fails the condition $C > 0$ for any value of the parameters.

For P_2, we have $C > 0$ when the equilibrium points exist. For $A > 0$, is necessary that $c \ge 2a$ or ($c \in (a, 2a)$ and $b < c-a$). The crucial point is the last condition: $AB > C$. After some algebra, we obtain the necessary and sufficient condition $-2a + 2b + 2a^2b + a^2c - ac^2 - a(c-a)K > 0$. For it to hold, first it is necessary that $-2a + 2b + 2a^2b + a^2c - ac^2 > 0$. Or, equivalently,

$$b > b_1(a,c) := \frac{a(2 + c(c-a))}{2(1+a^2)}.$$

Also, it is required that

$$4(1+a^2)^2b^2 - 4a(2 + 2a^2 - a^4 - ac + a^3c + c^2)b + 4a^2(1 + c(c-a)) > 0. \tag{4}$$

If $c < -a^3 + 2\sqrt{a^2+a^4}$, then condition (4) is satisfied for all b. If $c = -a^3 + 2\sqrt{a^2+a^4}$, then there is a number $b_H(a,c)$ such that condition (4) is true for all $b \ne b_H(a,c)$. Finally, if $c > -a^3 + 2\sqrt{a^2+a^4}$, then there are two numbers $b_h(a,c) < b_H(a,c)$, and inequality (4) is satisfied for $b < b_h(a,c)$ or $b > b_H(a,c)$. But, as $b_h(a,c) < b_1(a,c)$, the only valid situation is $b > b_H(a,c)$.

If $c \in (a, 2a)$, then $b_1(a,c) < c - a$ implies that $c > a + 2/a > -a^3 + 2\sqrt{a^2+a^4}$. So, $b_H(a,c)$ exists, and it is greater than $c - a$. Therefore, it is necessary that $c \ge 2a (> -a^3 + 2\sqrt{a^2+a^4}$ for positive a).

Thus, we need $c \geq 2a$ and $\max(b_1(a,c), b_H(a,c)) < b < b_E(a,c)$. But, $b_1(a,c) < b_E(a,c) \iff (a,c) \in S_1 \cup S_2$. And $b_H(a,c) \leq b_E(a,c)$ if $b_H(a,c)$ exists (with $b_H(a,c) = b_E(a,c) \iff c = 2a$ or $c = 2a/(a^2-1)$). Besides, $b_1(a,c) < b_H(a,c)$ in $S_1 \cup S_2$. This fact completes the proof. □

In Fig. 1, we show both surfaces, b_{H} and b_{E}. In picture A, we provide the three regions defined by both surfaces, the region of linear stability of P_2 (R1), the region with two unstable equilibrium points (R2), and the region without equilibrium points (R3). We highlight the curve intersection of both surfaces with green. Two detailed figures for the fixed value of $a = 0.2$ are shown in plots B and C (a magnification of B). A picture with a larger domain is shown in plot D, with the intersection of both surfaces on green. In plot E, we show the domain of definition on the (a, c) plane of the stable region R1. Finally, in plot F1 we show for $a = 0.5$ the curves b_{H} and b_{E}, and in F2, F3, and F4 we show for fixed values of a the difference $b_{\mathrm{E}} - b_{\mathrm{H}}$, giving us an idea of how close they are when $a > 1$ approaches the limit value $a_1 \equiv \sqrt{2}$. Another important remark is that for $a > a_1$ point P_2 is always unstable, and when $1 < a \leq a_1$ there is a finite interval on c on which P_2 is linearly stable (and so both surfaces intersect twice for these values of a) and for $0 < a \leq 1$ the interval is unbounded (see plot E).

From plots C, F1, F2, F3, and F4 we see that both surfaces, b_{E} and b_{H}, are tangent at the intersection points. This affirmation can be easily proved, since we have the explicit expressions; in fact, it has been practically demonstrated in the proof of Proposition 1 (also, this is known from the literature [12] about these codimension two points using normal form theory).

Proposition 2. *At the limit curves* $\{c = 2a, b = a\}$ *and* $\left\{c = \frac{2a}{a^2-1}, b = \frac{a}{(a^2-1)^2}\right\}$, *the surfaces* $b = b_{\mathrm{E}}(a,c)$ *and* $b = b_{\mathrm{H}}(a,c)$ *are tangent.*

3. Local bifurcations of equilibria

In this section, we analyze some of the codimension one, two, and three bifurcations of the equilibria. Clearly, the conditions of the existence of the equilibria $b = b_{\mathrm{E}}(a,c)$ give a surface of fold (saddle–node or tangent) bifurcations. The above analysis of the stability of the P_2 equilibrium point already gives some hints concerning the analysis of the Andronov–Hopf bifurcation of such a point. This bifurcation gives one mechanism of creation of limit cycles around P_2. In the literature, there are other studies about the Hopf bifurcation of the Rössler system [4,7–9,13–16].

Proposition 3. *The equilibrium point* P_2 *presents an Andronov–Hopf bifurcation at the parameter surface*

- $b = b_{\mathrm{H}}(a,c)$ *when* $c > 2a$ *and* $a \leq a_0 \equiv 1$,
- $b = b_{\mathrm{H}}(a,c)$ *when* $2a < c < \frac{2a}{a^2-1}$ *and* $a_0 < a < a_1 \equiv \sqrt{2}$,

where $b_{\mathrm{H}}(a,c)$ *is defined by* (3).

Proof. The conditions for the existence of the Andronov–Hopf bifurcation (after imposing the existence of two conjugate imaginary roots of the characteristic polynomial) are, on a general third-degree polynomial, that $AB = C$ and $B > 0$ (which occurs if $AC > 0$). In our problem, both conditions only occur for $A, C > 0$, and so we recover the first two RHC conditions that give the Andronov–Hopf bifurcation surface. Note that we also have to check the nondegeneracy condition $l_1(0) \neq 0$ (with $l_1(0)$ the first Lyapunov coefficient of the dynamical system near equilibrium), but this will be studied below to classify the type of Hopf bifurcation, and the transversality condition is satisfied when the parameters change on crossing the surface of the Hopf bifurcation (and not tangentially). □

Note that we are in a three-dimensional system, and thus to have an Andronov–Hopf bifurcation it is not necessary to change the stability properties; therefore P_1 can also experience such a bifurcation. By imposing the conditions for the Andronov–Hopf bifurcation (two imaginary eigenvalues) on P_1, and after some tedious algebra, we obtain the proposition.

Proposition 4. *The equilibrium point* P_1 *presents an Andronov–Hopf bifurcation at the parameter surfaces*

- $b = b_{\mathrm{H}}(a,c)$ *when* $-a^3 + 2\sqrt{a^4+a^2} < c < 2a$ *for* $a \leq a_1 \equiv \sqrt{2}$,
- $b = b_{\mathrm{H}}(a,c)$ *when* $-a^3 + 2\sqrt{a^4+a^2} < c < \frac{2a}{a^2-1}$ *for* $a_1 < a \leq a_2 \equiv \sqrt{3}$,
- $b = b^*_{\mathrm{H}}(a,c)$ *when* $c > -a^3 + 2\sqrt{a^4+a^2}$ *for* $a \leq a_2$,
- $b = b^*_{\mathrm{H}}(a,c)$ *when* $c > \frac{2a}{a^2-1}$ *for* $a \geq a_2$,

where $b_{\mathrm{H}}(a,c)$ *is defined by* (3) *and*

$$b^*_{\mathrm{H}}(a,c) := \frac{a\left(2 - a^4 + ca^3 + 2a^2 - ca + c^2 - (c-a)\sqrt{a^6 - 4a^4 + 2ca^3 - 4a^2 + c^2}\right)}{2\left(a^2+1\right)^2}.$$

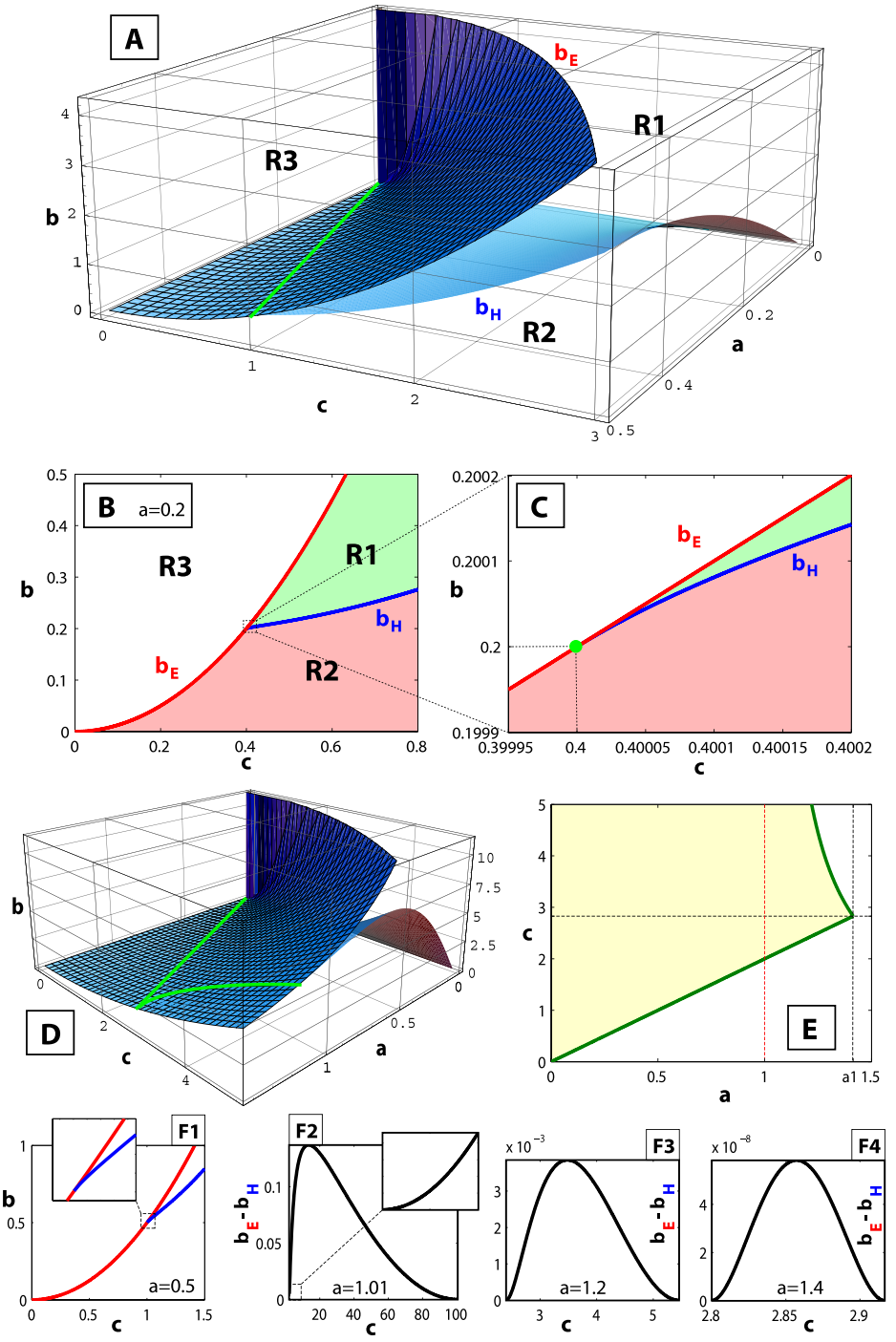

Fig. 1. Domain of stability of the P_2 equilibrium point.

The point $a_1 \equiv \sqrt{2}$ is given by the intersection of the curves $c = 2a$ and $c = \frac{2a}{a^2-1}$, and $a_2 \equiv \sqrt{3}$ of the curves $c = \frac{2a}{a^2-1}$ and $c = -a^3 + 2\sqrt{a^4 + a^2}$ in the (a, c) plane. The point $a_0 \equiv 1$ was defined previously for the point P_2. With these curves and points we can establish different regions in the (a, c) plane, depending on the existence or not of Andronov–Hopf bifurcations. In Fig. 2, we show in the picture on the top all the different possibilities. The color codes are as follows: yellow when there is a value of b with a Hopf bifurcation of P_1 and another one of P_2, green for two values of b with a Hopf bifurcation of P_1, blue for one value of b with a Hopf bifurcation of P_1, and white for no Hopf bifurcations at any value of b. In region A ($0 < a \leq a_0$), there are Andronov–Hopf bifurcations for both equilibria and, once a is fixed, the interval on the parameter

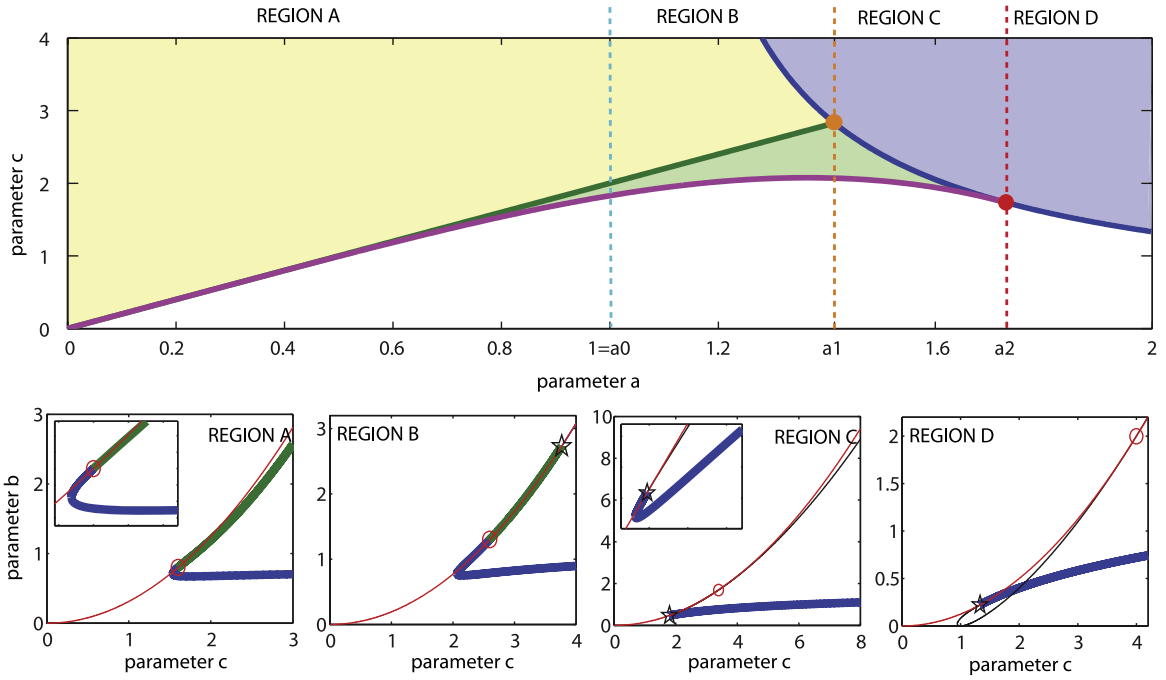

Fig. 2. (Top) Domain of existence on the plane (a, c) of the Andronov–Hopf bifurcations of the P_1 and P_2 equilibrium points. (Bottom) Schematic possibilities for fixed values of a of the Andronov–Hopf bifurcation curves.

c is unbounded. In the magnification of region A with fixed a, we show the curve $b = b_{\mathrm{E}}(a, c)$ in red, which in the upper part defines the region without equilibria. The tangent intersections of b_{E} and b_{H} or b_{H}^* are pointed out with a red circle and a black star. In region A, there is just one intersection point. At this point, both equilibria are the same, and there are two branches of Andronov–Hopf bifurcations, one for each equilibrium. In green is the one for P_2 and in blue is that for P_1. Note that both branches are unbounded. In region B ($a_0 < a < a_1$), there are also Andronov–Hopf bifurcations for both equilibria but, once a is fixed, the interval of the parameter c is unbounded for P_1 but is bounded for P_2, because now there are two tangent intersections. In the magnification of region B, once a is fixed, we see two tangent intersections giving a bounded interval in c for the bifurcation. The interval decreases in size when a grows, and at $a = a_1$ both intersection points overlap, and there is no Andronov–Hopf bifurcation for P_2. In regions C ($a_1 < a < a_2$) and D ($a_2 < a$), there is an Andronov–Hopf bifurcation just for P_1. In region C, once a is fixed, there are two values of b where the bifurcation occurs in the green region of the top plot of Fig. 2. In region D, there is just one value in all the region.

The study of the type of Andronov–Hopf bifurcation (subcritical or supercritical) is determined by the sign of the first Lyapunov coefficient $l_1(0)$ of the dynamical system near equilibrium. There are several approaches to compute this coefficient, such as the Bautin formula [17] or the one used here [12]. By writing our differential system, after a translation of the equilibrium point to the origin, as $\dot{x} = A_0 x + \frac{1}{2}B(x, x)$ with $B(x, y)$ a bilinear form that gives the quadratic terms, we obtain [12]

$$l_1(0) = \frac{1}{2\omega_0}\mathrm{Re}\left\{-2\langle p, B(q, A_0^{-1}B(q, \bar{q}))\rangle + \langle p, B(\bar{q}, (2i\omega_0 I_n - A_0)^{-1}B(q, q))\rangle\right\},$$

where $q \in \mathbb{C}^3$ is a unitary complex eigenvector of A_0 corresponding to the eigenvalue $i\omega_0$, and p is an adjoint eigenvector ($A_0^{\top}p = -i\omega_0 p$) satisfying $\langle p, q\rangle = \bar{p}^{\top}q = 1$. If $l_1(0)$ is positive then the Andronov–Hopf bifurcation is subcritical, and if $l_1(0)$ is negative then the Andronov–Hopf bifurcation is supercritical. As an analytical study of l_1 is too cumbersome, for this problem we have done a numerical study by computing $l_1(0)$ for a grid of 1000×1000 parameter values on the rectangle $(a, c) \in [0, 2.25] \times [0, 5]$. In Fig. 3, we present the numerical values of $l_1(0)$. The surface on the top is the surface of the Andronov–Hopf bifurcation for P_2, and the color texture is the value of $l_1(0)$. In this case, the value is always negative, and thus the Hopf bifurcation is supercritical. The surface on the bottom is the surface of the Andronov–Hopf bifurcation for P_1. In this case, the value can be positive (subcritical Hopf) or negative, and there is a curve of points where $l_1(0) = 0$, which is a curve of a codimension two bifurcation: the generalized-Hopf or Bautin bifurcation [12]. The curve is pointed out with a black curve on the bottom surface. The small plots on the right of Fig. 3 provide the view of the domain of the surfaces on the (a, c) plane. Note that the surface for P_1 has a loop, and in one region (the region with green color on top plot of Fig. 2) there are two values of b with an Andronov–Hopf bifurcation. At the points of the generalized-Hopf bifurcation, it is interesting to compute also the second Lyapunov coefficient $l_2(0)$ [12]. Our numerical simulations give negative values of $l_2(0)$ at any

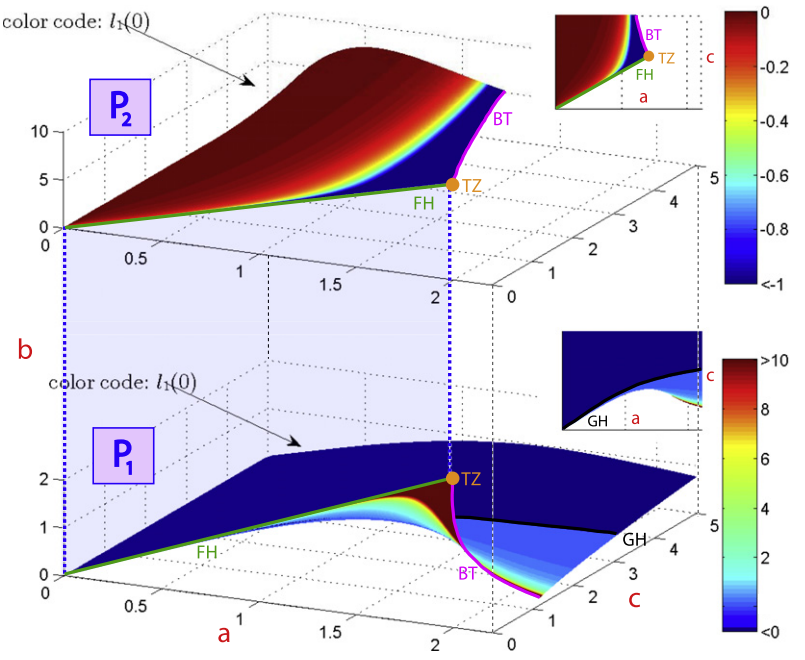

Fig. 3. Andronov–Hopf bifurcation surfaces using as the color texture the first Lyapunov coefficient $l_1(0)$.

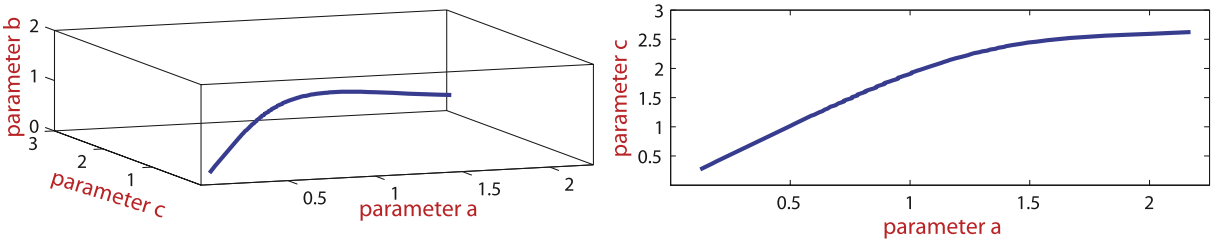

Fig. 4. Curve of the generalized-Hopf bifurcation.

point of the generalized-Hopf bifurcation for $a \in [0, 2.25]$, and therefore there are no more degeneracies in this interval. The numerical results permit us to provide a conjecture concerning the behavior of the Andronov–Hopf bifurcation.

Conjecture 5. *The equilibrium point P_2 presents a supercritical Andronov–Hopf bifurcation at the parameter surface given by Proposition 3. The equilibrium point P_1 has a curve of generalized-Hopf bifurcation that divides the parameter surface $b = b^*_{\mathrm{H}}(a, c)$ given by Proposition 4 into two regions, one of subcritical and the other of supercritical Andronov–Hopf bifurcations.*

In Fig. 4, we show the computed curve of the generalized-Hopf bifurcation. A mean-squares approximation of the values of the points of the curve (the parameter b is obtained from Proposition 4) is given by

$$c(a)_{\mathrm{GH}} \simeq 0.242 \cdot a^4 - 1.215 \cdot a^3 + 1.376 \cdot a^2 + 1.432 \cdot a + 0.0717, \quad a \in [0, 2.25], \qquad \|\mathrm{error}\|_2 = 0.057. \tag{5}$$

The surfaces for P_1 and P_2 coincide when they intersect tangentially with b_{E}, and since this is when both equilibria collide we have a curve of another codimension two bifurcation, in this case, as the third eigenvalue is zero (the spectrum along this curve is $\{0, \pm\mathrm{i}\sqrt{2 - a^2}\}$, $a \in [0, a_1 \equiv \sqrt{2})$), a fold-Hopf bifurcation (also called a saddle-Hopf, zero-Hopf, or Gavrilov–Guckenheimer bifurcation). The equations of this curve are

$$c = 2a, \qquad b = a, \quad \text{for } a \in [0, a_1),$$

and its plot on the (a, c) plane is the green straight line in the top plots of Figs. 2 and 3. There is another intersection curve, when the Andronov–Hopf bifurcation surfaces for P_1 or P_2 touch b_{E} (but not both at the same time), giving a curve of equilibrium points with two zero eigenvalues. This defines another codimension two bifurcation, the Bogdanov–Takens (BT) or double-zero bifurcation, with equations for both equilibria given by

$$c = \frac{2a}{a^2 - 1}, \qquad b = \frac{a}{(a^2 - 1)^2}, \quad \text{for } a \in [a_0, +\infty),$$

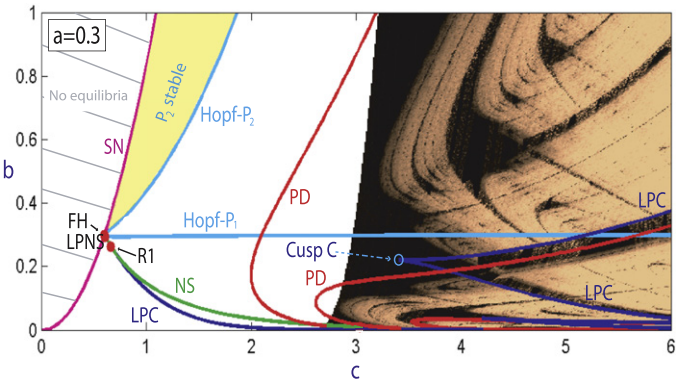

Fig. 5. Bifurcation curves over MLE–OFLI2 diagrams on the (c, b) plane for the parameter $a = 0.3$.

and its plot is the pink curve on the top plots of Fig. 3. In the interval $a \in [a_0, a_1)$, it corresponds to a BT bifurcation of P_2; and, for $a \in [a_1, +\infty)$, to P_1. Along the BT curve, the spectrum is given by $\{0, 0, a(a^2 - 2)/(a^2 - 1)\}$. Note that, at the BT and fold-Hopf bifurcations, the surfaces of the fold and Hopf bifurcations, b_E and b_H, are tangential, as predicted by the theory [12] (and by Proposition 2).

The intersection of the Bogdanov–Takens and the fold-Hopf bifurcations give rise to a set of parameters $(a, b, c) = (\sqrt{2}, \sqrt{2}, 2\sqrt{2})$ of a bifurcation of codimension three, a triple-zero bifurcation [18] (TZ in Fig. 3).

Finally, we remark that the fold-Hopf bifurcation of three-dimensional vector fields generically [12,19,20] shows Shilnikov bifurcations of equilibria [21], which is a complicated homoclinic phenomenon that may cause the birth of Shilnikov strange attractors. We also note that the BT bifurcations also indicate the presence of a branch of homoclinic bifurcations [21] (see the next section for an example).

4. Regular and chaotic regions, connections of bifurcation curves

In [10], the authors develop a complete study of the local and global bifurcations of limit cycles. Besides, they study the different regions in the three-parametric space where chaotic behavior may be expected. This was done using the maximum Lyapunov exponent (MLE) [22] and the OFLI2 Chaos Indicator [23] (see [10] for details). We remark that a positive value of the MLE is usually associated with a chaotic behavior for bounded orbits.

Here we add to the MLE–OFLI2 diagrams some bifurcation curves, as done in Fig. 5, that have been computed using AUTO [24] and MATCONT [25]. In the picture, the MLE–OFLI2 results are coded in black for the regular region and in a scale of orange for the chaotic region, whereas shown in white is the escape region which corresponds to escape orbits for the chosen initial conditions. Note that the figure is on the (c, b) plane for $a = 0.3$, which corresponds to region A of Fig. 2. We have calculated different bifurcation curves of equilibria and limit cycles. For the equilibria we show the fold or saddle–node bifurcation (SN) (given by equation $b = b_E$) and the Andronov–Hopf bifurcation curves for the points P_1 and P_2, and also the fold-Hopf codimension two point (FH) located at the point $(b, c) = (0.3, 0.6)$. Between the SN and the Hopf-P_2 curves we have a region where the P_2 equilibrium is stable, and also there is a region without equilibrium points. For the periodic orbits, we show the curves corresponding to some period-doubling bifurcations (PD), Neimark–Sacker (NS) bifurcation, saddle–node bifurcation of cycles (LPC), and the codimension two points given by the cusp bifurcation of cycles (Cusp C) where two branches of LPC bifurcations meet tangentially, the Fold–Neimark–Sacker bifurcation (LPNS) and the strong resonance $1 : 1$ (R1, with triple multiplier 1). Most of the bifurcations occur in the escape region, and so these bifurcations have a limited influence just for points close to the bifurcated structures, but the rest of the initial conditions escape to infinity. Note that some of these bifurcation curves coincide with the limits of the different chaotic structures that we have identified with the MLE–OFLI2 diagram; therefore, a good correspondence is obtained between both of them, giving us good confidence for the results.

Finally, in Fig. 6, we have computed a homoclinic bifurcation curve of orbits around P_2 (HB2) and some local bifurcations of limit cycles and equilibria on the (a, c) plane for $b = 0.2$. The point -1- serves as an organization point [10], and it is a point where a double real determining eigenvalue codimension two point occurs (in this case double real leading unstable eigenvalues $\lambda_2 = \lambda_3 > 0$, leading to a saddle to saddle-focus transition). This degenerated case was studied by Belyakov [26], and there are two bundles each consisting of an infinite number of bifurcation curves of homoclinic orbits and fold bifurcations of periodic orbits. The bundles extend from the bifurcation point to the saddle-focus region (in our case to the left). We also show a Bogdanov–Takens (or double-zero) bifurcation point (BT). The diagrams below represent several routes connecting the different Hopf bifurcation curves. Note that route C begins on the right at a subcritical Andronov–Hopf bifurcation curve of P_1 (point -6-) but finishes on the Homoclinic curve (point -5-) of orbits around P_2 (HB2), which is born at the Bogdanov–Takens codimension two point. Route B is created at a supercritical Hopf curve (point -2-) of P_2, bounces at the saddle–node bifurcation of cycles (LPC) (point -4-), and after going through a period-doubling bifurcation, finishes in

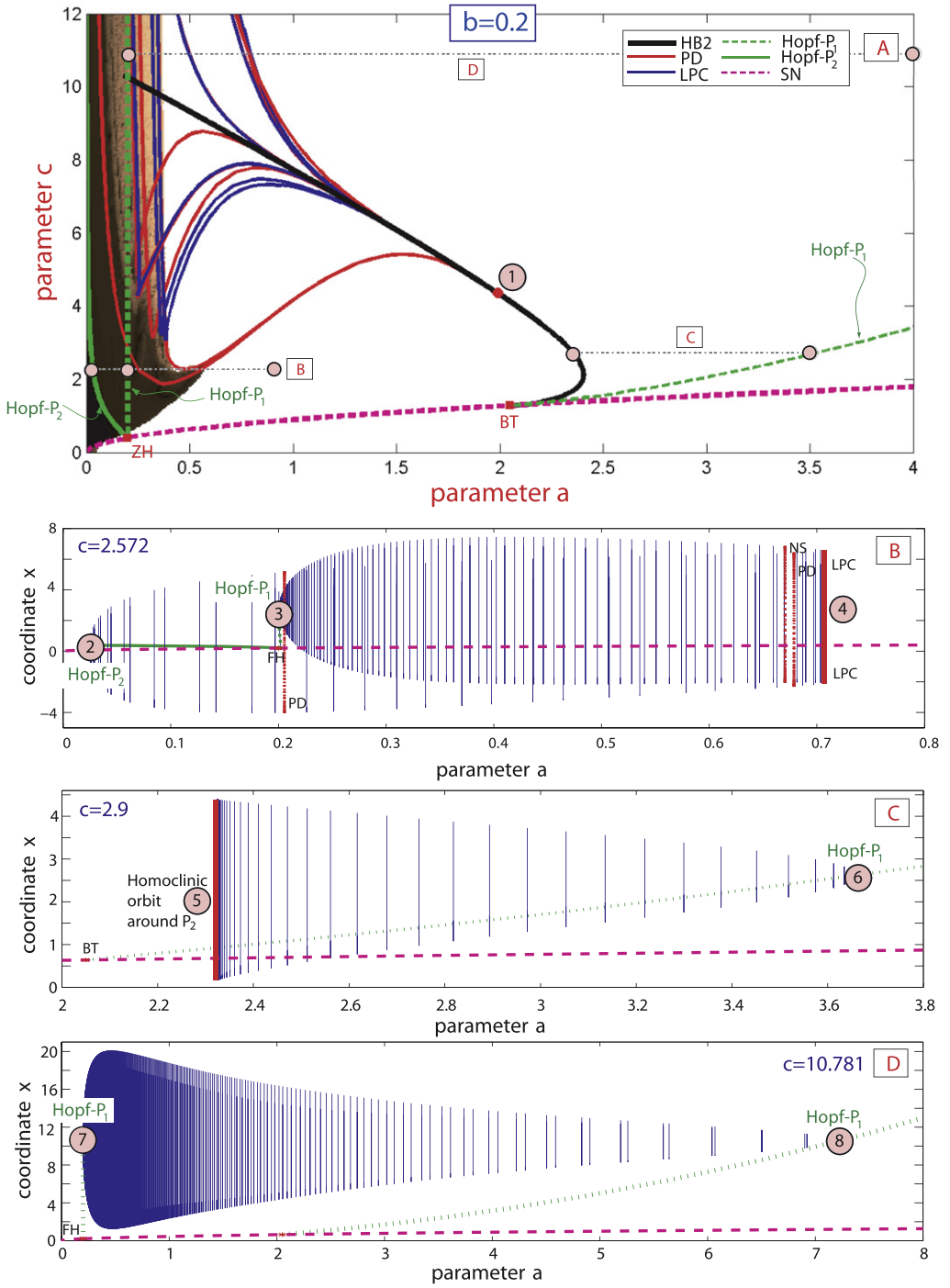

Fig. 6. Top: Homoclinic bifurcation curve and some local bifurcations of limit cycles and equilibria on the (a, c) plane for $b = 0.2$. Bottom: routes connecting the different Hopf bifurcation curves.

the second supercritical Hopf bifurcation of P_1, point -3- (each Hopf bifurcation curve corresponds to different equilibria). The last route, namely route D, starts on the left Hopf curve (point -7-) and is able to reach the other Hopf curve to the right (point -8-) since it has a value of the parameter c well above the homoclinic curve, so it does not touch the equilibrium point and continues to the other Hopf bifurcation, where it disappears (note that in this case both Hopf bifurcations correspond to the same point P_1, but one is supercritical, on the left, and the other one subcritical, on the right). This analysis gives us a complete idea of the connections of cycles between the Hopf bifurcation curves.

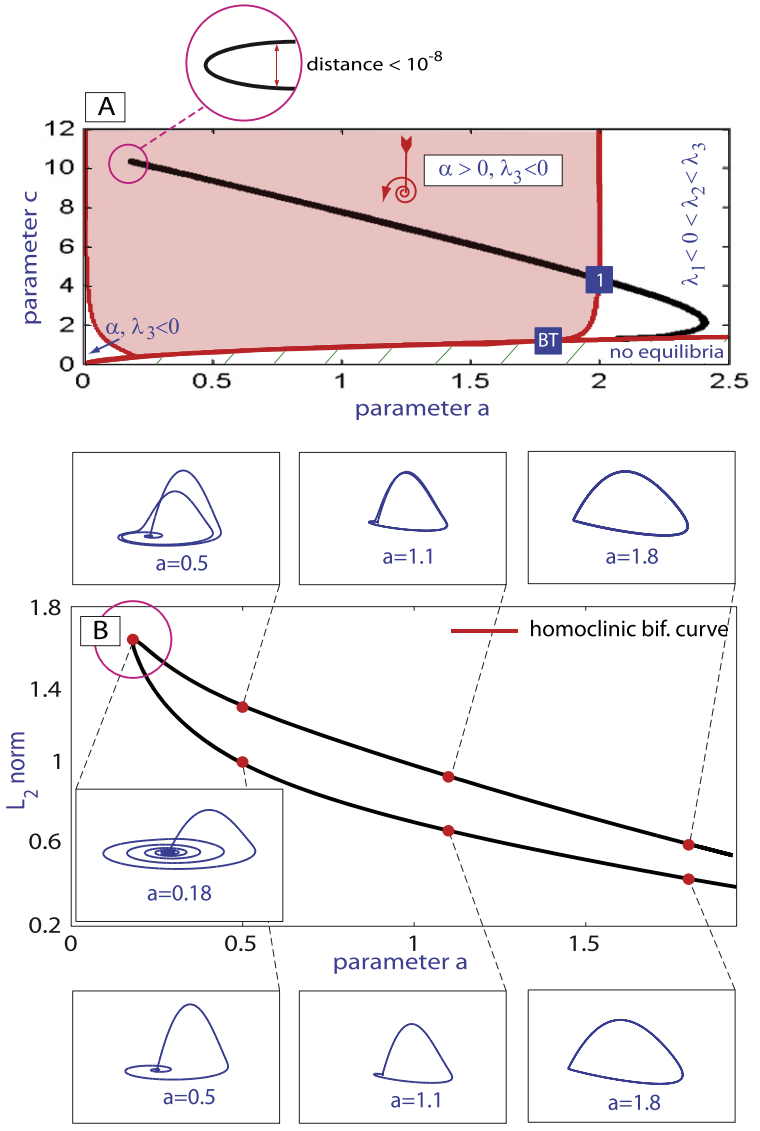

Fig. 7. (A) Type of equilibria on the (a, c) plane for $b = 0.2$. (B) Transformation of homoclinic orbits to the saddle-focus, P_2, in the Rössler system. The AUTO L_2-norm of the orbit is plotted against the bifurcation parameter a. The turning point terminates two branches: the bottom one corresponds to the primary homoclinic loop, while the top one corresponds to the secondary loop with an additional round. Homoclinic orbits are sampled at the indicated points.

According to the Shilnikov results, depending on the magnitudes of the characteristic exponents of the saddle-focus equilibrium P_2, the homoclinic bifurcation can give rise to the onset of either rich complex or trivial dynamics in the system [21,27,28]. If a homoclinic orbit exists on a saddle-focus equilibrium with eigenvalues $\lambda_{1,2} = \alpha \pm i\beta, \lambda_3$, with $\beta \neq 0$, and satisfies the condition $\mid \alpha/\lambda_3 \mid < 1$, there exists a countable number of Smale horseshoes in the vicinity of the homoclinic orbit. In Fig. 7, we show on the plane (a, c) the character of the equilibrium P_2 for $b = 0.2$ depending on the type of the eigenvalues ($\lambda_{1,2} = \alpha \pm i\beta$ and λ_3 in the case of a saddle-focus or $\lambda_1, \lambda_2, \lambda_3 \in \mathbb{R}$) of the Jacobian matrix, where the region that satisfies the Shilnikov hypothesis is noted. At $b = 0.2$, the homoclinic orbits belong to the equilibrium point P_2 and only satisfies the Shilnikov hypothesis on P_2 in a part of the homoclinic bifurcation curve (see Fig. 7) where we have homoclinic orbits to a saddle-focus. The (thick black) bifurcation curve in Fig. 7(A) corresponds to a formation of the primary homoclinic orbit to the saddle-focus, P_2, of topological type (1, 2), i.e. with one-dimensional stable and two-dimensional unstable manifolds, in the Rössler model (1). The cases under consideration meet the Shilnikov conditions, and hence the existence of a single homoclinic orbit implies chaotic dynamics in the models within the parameter range in the presented diagrams. In order to examine the corresponding homoclinic bifurcation curve in detail [11], we plot (Fig. 7(B)) the bifurcation curve in terms of the L_2-norm [24] of the homoclinic orbit against the bifurcation values of the parameter a. For periodic solutions $U(t)$, the L_2-norm is defined as

$$\|U\|_2 = \sqrt{\int_0^1 \|U(t)\|^2 dt},$$

where the independent variable t is scaled to [0, 1]. This diagram reveals that what appears to be as a single bifurcation curve has two branches: the bottom one corresponds to the primary homoclinic loop, while the top one corresponds to the secondary loop with an additional round. This curve has a U-shape, with a very small distance of both branches in the parametric plane [29].

5. Conclusions

In this paper, we have shown the combined use of analytical and numerical techniques to compute bifurcation curves of equilibria of simple chaotic systems. The techniques have been applied to the detailed study of different aspects of the paradigmatic Rössler model. We provide analytical formulas for the stability of the equilibria as well as some of their codimension one, two, and three bifurcations.

We have carried out a complete study of the Andronov–Hopf bifurcation, establishing explicit formulas for its location and studying its character numerically, determining a curve of generalized-Hopf bifurcation, where the Hopf bifurcation changes from subcritical to supercritical.

We have also studied some routes among the different Hopf bifurcation curves and how these routes are influenced by the local and global bifurcations of limit cycles, namely the fold and period-doubling bifurcations on one side and the existence of homoclinic orbits on the other. Finally, we have shown the U-shape of the homoclinic bifurcation curve at $b = 0.2$.

A table with the major qualitative and numerical results summarized is given below.

EP	Property	Result
P_1	Always unstable	Proposition 1
P_2	Linearly stable in some cases	Proposition 1
P_1	Andronov–Hopf bifurcation	Proposition 4
P_2	Andronov–Hopf bifurcation	Proposition 3
P_1	Andronov–Hopf bifurcation is supercritical or subcritical	Conjecture 5
P_2	Andronov–Hopf bifurcation is supercritical	Conjecture 5
P_1	Generalized-Hopf bifurcation curve	Eq. (5)
P_1, P_2	Fold-Hopf bifurcation	$c = 2a, b = a,$ for $a \in [0, \sqrt{2})$
P_1	Bogdanov–Takens bifurcation	$c = 2a/(a^2-1), b = a/(a^2-1)^2,$ for $a \in [\sqrt{2}, +\infty)$
P_2	Bogdanov–Takens bifurcation	$c = 2a/(a^2-1), b = a/(a^2-1)^2,$ for $a \in [1, \sqrt{2})$
P_1, P_2	Triple-zero bifurcation	$(a, b, c) = (\sqrt{2}, \sqrt{2}, 2\sqrt{2})$
P_2 + hom	Belyakov point in homoclinic curve ($b = 0.2$)	$(a, b, c) \approx (1.9910, 0.2, 4.3508)$
P_2 + hom	Turning point (U-shape) of the homoclinic curve ($b = 0.2$)	$(a, b, c) \approx (0.1798, 0.2, 10.3084)$

In this table, we indicate in the first column the corresponding equilibrium point (EP), in the second one the property that we have found, and in the last column we put where the results relative to that property can be found in the text. If the result is a numerical result, we put the approximate equation of the curve or the approximate coordinates of the point.

Acknowledgments

The authors R.B., A.D., and S.S. were supported by the Spanish Research project MTM2009-10767, and the author F.B. was supported by the Spanish Research project AYA2008-05572/ESP.

References

[1] O.E. Rössler, An equation for continuous chaos, Phys. Lett. A 57 (5) (1976) 397–398.
[2] A. Algaba, E. Freire, E. Gamero, A.J. Rodríguez-Luis, Resonances of periodic orbits in Rössler system in presence of a triple-zero bifurcation, Internat. J. Bifur. Chaos 17 (6) (2007) 1997–2008.
[3] V. Castro, M. Monti, W.B. Pardo, J.A. Walkenstein, E. Rosa Jr., Characterization of the Rössler system in parameter space, Internat. J. Bifur. Chaos 17 (3) (2007) 965–973.
[4] R. Genesio, G. Innocenti, F. Gualdani, A global qualitative view of bifurcations and dynamics in the Rössler system, Phys. Lett. A 372 (2008) 1799–1809.
[5] J. Llibre, C. Valls, Formal and analytic integrability of the Rössler system, Internat. J. Bifur. Chaos 17 (9) (2007) 3289–3293.
[6] S. Nikolov, V. Petrov, New results about route to chaos in Rössler system, Internat. J. Bifur. Chaos 14 (1) (2004) 293–308.
[7] L. Gardini, Hopf bifurcations and period-doubling transitions in Rössler model, Nuovo Cimento B (11) 89 (2) (1985) 139–160.

[8] K.E. Starkov, K.K. Starkov Jr., Localization of periodic orbits of the Rössler system under variation of its parameters, Chaos Solitons Fractals 33 (5) (2007) 1445–1449.
[9] M.T. Terëkhin, T.L. Panfilova, Periodic solutions of the Rössler system, Izv. Vyssh. Uchebn. Zaved. Mat. 8 (1999) 70–73.
[10] R. Barrio, F. Blesa, S. Serrano, Qualitative analysis of the Rössler equations: bifurcations of limit cycles and chaotic attractors, Physica D 238 (2009) 1087–1100.
[11] R. Barrio, F. Blesa, S. Serrano, A. Shilnikov, Global organization of spiral structures in biparameter space of dissipative systems with Shilnikov saddle-foci, Phys. Rev. E 84 (2011) 035201.
[12] Y.A. Kuznetsov, Elements of Applied Bifurcation Theory, 3rd ed., in: Applied Mathematical Sciences, vol. 112, Springer-Verlag, New York, 2004.
[13] Z. Galias, Counting low-period cycles for flows, Internat. J. Bifur. Chaos 16 (10) (2006) 2873–2886.
[14] J. Llibre, C.A. Buzzi, P.R.D. Silva, 3-dimensional Hopf bifurcation via averaging theory, Discrete Contin. Dyn. Syst. 17 (3) (2007) 529–540.
[15] N.A. Magnitskii, S.V. Sidorov, Transition to chaos in nonlinear dynamical systems described by ordinary differential equations, Comput. Math. Model. 18 (2) (2007) 128–147.
[16] P. Yu, G. Chen, Hopf bifurcation control using nonlinear feedback with polynomial functions, Internat. J. Bifur. Chaos 14 (5) (2004) 1683–1704.
[17] N.N. Bautin, Criteria for unsafe and safe bounds of a region of stability, Akad. Nauk SSSR. Prikl. Mat. Meh. 12 (1948) 691–728.
[18] E. Freire, E. Gamero, A.J. Rodríguez-Luis, A. Algaba, A note on the triple-zero linear degeneracy: normal forms, dynamical and bifurcation behaviors of an unfolding, Internat. J. Bifur. Chaos 12 (12) (2002) 2799–2820.
[19] H. Broer, C. Simó, R. Vitolo, Bifurcations and strange attractors in the Lorenz-84 climate model with seasonal forcing, Nonlinearity 15 (4) (2002) 1205–1267.
[20] J. Guckenheimer, P. Holmes, Nonlinear Oscillations, Dynamical Systems, and Bifurcations of Vector Fields, in: Applied Mathematical Sciences, vol. 42, Springer-Verlag, New York, 1990.
[21] L.P. Shilnikov, A.L. Shilnikov, D. Turaev, L.O. Chua, Methods of Qualitative Theory in Nonlinear Dynamics. Part II, World Scientific Publishing Co. Inc., 2001.
[22] J. Argyris, G. Faust, M. Haase, An Exploration of Chaos, Texts on Computational Mechanics, VII, North-Holland Publishing Co., Amsterdam, 1994.
[23] R. Barrio, Sensitivity tools vs. Poincaré sections, Chaos Solitons Fractals 25 (3) (2005) 711–726.
[24] E.J. Doedel, R.C. Paffenroth, A.R. Champneys, T.F. Fairgrieve, Y.A. Kuznetsov, B.E. Oldeman, B. Sandstede, X.J. Wang, Auto2000: Continuation and bifurcation software for ordinary differential equations, 2000. URL: http://cmvl.cs.concordia.ca/.
[25] A. Dhooge, W. Govaerts, Y.A. Kuznetsov, MATCONT: a MATLAB package for numerical bifurcation analysis of ODEs, ACM Trans. Math. Software 29 (2) (2003) 141–164.
[26] L.A. Belyakov, The bifurcation set in a system with a homoclinic saddle curve, Mat. Zametki 28 (6) (1980) 911–922. 962.
[27] P. Gaspard, G. Nicolis, What can we learn from homoclinic orbits in chaotic dynamics? J. Stat. Phys. 31 (3) (1983) 499–518.
[28] L.P. Shilnikov, A case of the existence of a countable number of periodic motions, Sov. Math. Dokl. 6 (1965) 163.
[29] R. Vitolo, P. Glendinning, J.A.C. Gallas, Global structure of periodicity hubs in Lyapunov phase diagrams of dissipative flows, Phys. Rev. E 84 (2011) 016216.